AGU ADVANCING EARTH AND SPACE SCIENCE

Geophysical Research Letters

RESEARCH LETTER
10.1029/2021GL093440

Robust Asymmetry of the Future Arctic Polar Vortex Is Driven by Tropical Pacific Warming

Shinji Matsumura[1], **Koji Yamazaki**[2], **and Takeshi Horinouchi**[1]

[1]Faculty of Environmental Earth Science, Hokkaido University, Sapporo, Japan, [2]Arctic Research Center, Hokkaido University, Sapporo, Japan

Key Points:

- The Arctic stratospheric cooling in the future is most pronounced over Eurasia, whereas over North America stratospheric warming occurs
- Tropical Pacific warming takes the place of Arctic sea ice loss as the dominating forcing of the polar vortex
- The asymmetric polar vortex could act to increase the cold extreme events over mid- to high-latitudes of Eurasia in the near future

Supporting Information:

Supporting Information may be found in the online version of this article.

Correspondence to:

S. Matsumura,
matsusnj@ees.hokudai.ac.jp

Citation:

Matsumura, S., Yamazaki, K., & Horinouchi, T. (2021). Robust asymmetry of the future Arctic polar vortex is driven by tropical Pacific warming. *Geophysical Research Letters*, *48*, e2021GL093440. https://doi.org/10.1029/2021GL093440

Received 22 MAR 2021
Accepted 22 MAY 2021

Abstract The future stratosphere is globally dominated by a strong radiative cooling due to the increase in greenhouse gases. However, we find that over North America, the Arctic stratospheric cooling is suppressed or rather warming occurs, whereas over Eurasia stratospheric cooling is most pronounced, leading to an asymmetric polar vortex, based on 21st century climate model simulations. There are many causes that drive polar vortex variability, which make future projections highly uncertain. Our model simulations demonstrate that tropical warming induces the asymmetric polar vortex. The eastern equatorial Pacific warming causes eastward-shifted teleconnection with a deepened Aleutian low, which strengthens the polar vortex over Eurasia and weakens over North America by enhancing the vertical wave propagation into the stratosphere. The asymmetric polar vortex is projected to markedly develop in the 2030s, and so could affect winter surface climate over mid- to high-latitudes of Eurasia in the near future.

Plain Language Summary Recent cold extremes in northern mid-latitudes have seriously damaged economic and societal activities. It has been suggested that during the past three decades the Arctic stratospheric polar vortex has slightly shifted away from North America toward Eurasia associated with Arctic sea ice loss, favoring the cold extremes. Our study shows that in a few decades, such extreme weather events might further increase or intensify due to the enhancement of the polar vortex asymmetry between North America and Eurasia. We found that the asymmetric polar vortex significantly develops in the 2030s and is robust throughout the late 21st century. The asymmetric polar vortex is caused by tropical ocean warming. These findings provide a new insight into Arctic climate changes and would help advance our understanding of ongoing mid-latitude climate change.

1. Introduction

The larger topographic and land-sea contrasts in the Northern Hemisphere (NH) produce stronger upward propagating planetary waves into the stratosphere than in the Southern Hemisphere (SH), causing the Arctic stratospheric polar vortex (hereafter polar vortex) to be more disturbed (Waugh et al., 2017). Recent weakening of the polar vortex (Garfinkel et al., 2017; Kretschmer et al. 2018; Seviour, 2017) is suggested to be associated with Arctic sea ice loss as a cause of recent Eurasian cooling (e.g., Kim et al., 2014; Nakamura et al., 2016), although the underlying mechanisms are yet inconclusive (Screen et al., 2018). In contrast, one recent study suggested that the polar vortex has strengthened since the 2000s associated with the North Pacific warming (Hu et al., 2018), which has opposing influences with Arctic sea ice loss (e.g., Kim et al., 2014; Nakamura et al., 2016; Peings & Magnusdottir, 2014; Sun et al., 2015). In particular, sea surface temperature (SST) is regarded as a major driver of polar vortex variability. El Niño Southern Oscillation (ENSO) affects the strength and variability of the polar vortex; El Niño events lead to a warming and weakening of the polar vortex (e.g., Domeisen et al., 2019; Garfinkel & Hartmann, 2008; Ineson & Scaife, 2009; Manzini et al., 2006)

Considering the characteristics of the polar vortex with a center over the pole (i.e., circumpolar westerly jet), many previous studies are based on the zonal mean fields. However, the polar vortex in February has slightly shifted away from North America toward Eurasia over the past three decades (Seviour, 2017; Zhang et al., 2016) contributing to slow down the stratospheric ozone recovery over the Eurasian continent (Zhang et al., 2018). This is suggestive of an importance of the polar vortex shift or its horizontal structure in the wavier NH than the SH. Under increased greenhouse gas emissions a globally averaged stratospheric cooling is expected (Manabe & Wetherald, 1975; Manzini et al., 2014), whereas this is suggested to be offset

over the Arctic by a strengthened Brewer-Dobson circulation (Domeisen et al., 2019; Karpechko & Manzini, 2017; Manzini et al., 2014), which make future projection on the polar vortex highly uncertain (Manzini et al., 2014; Screen et al., 2018; Simpson et al., 2018). Our study shows that the polar vortex continues to shift toward Eurasia due to tropical Pacific warming, having an asymmetric structure between North America and Eurasia.

2. Methods

2.1. Data and Analyses

We used Coupled Model Intercomparison Program Phase 5 (CMIP5) models (Taylor et al., 2012) (Table S1). Atmospheric data were horizontally interpolated onto a 2.5° × 2.5° grid and SST data were interpolated onto a 1° × 1° grid. For the historical and Representative Concentration Pathway (RCP) 8.5 scenarios the response to anthropogenic forcing is defined as the difference between the 2070–2099 period from the RCP8.5 run and the 1970–1999 period from the historical run. All data used in this study were averaged over the 30 CMIP5 models, except that geopotential height is based on 29 models (unavailable HadGEM2-CC data). This study focuses on boreal winter (December–February). All regression and correlation analyses are conducted after linear detrending. The significance test used in this study is a standard two-tailed *t* test.

2.2. AGCM Simulations

We made use of the simulations conducted in our earlier study that focuses on tropospheric midlatitude jet (Matsumura et al., 2019). All experiments use the Dennou-Club Planetary Atmospheric Model (DCPAM5) (Takahashi & DCPAM Devlopment Group, 2018) with 26 vertical layers extending to about 6.5 hPa and a spectral resolution of T85, roughly equivalent to 1.4° × 1.4°. Further description of the model is provided in Matsumura et al. (2019).

As stratospheric variability is dependent on a model's lid height, we confirmed the ability of the model to simulate it (Figure S1). The climatological zonal-mean jet is stronger than that in JRA55 reanalysis (Kobayashi et al., 2015), but its distribution is well reproduced. Despite the fact that many low-top models have strongly suppressed stratospheric variability compared with reanalysis data (Kim et al., 2017), our jet variability has a comparable magnitude with JRA55 reanalysis (approximately 8 m s^{-1}). The horizontal distribution and variability of the polar vortex are also well captured in this model. These results confirm that our low-top model is suitable for understanding changes in the polar vortex.

Four experiments were performed (Table S2). In HIST experiment, the model is forced globally with historical SST and sea ice distribution, while GLSST experiment is forced globally with RCP8.5 SST and sea ice distribution. AICE experiment is the same as HIST, except for RCP8.5 Arctic sea ice distribution. The GLSST and AICE responses are defined as the difference with HIST experiment. To obtain the atmospheric response due to mid- and low latitudes SST warming, we performed MLSST + AICE experiment, which is forced with RCP8.5 mid-latitude SST (north of 35°N: 15–35°N with linear tapering zones, so that RCP8.5 mid-latitude SST does not exceed the historical lower latitude SST) and Arctic sea ice distribution, but with historical conditions elsewhere. The mid-latitude SST warming (MLSST) response is estimated by subtracting AICE from MLSST + AICE experiment (Figure S2). Similarly, the difference between GLSST and MLSST + AICE experiments provides the atmospheric response due to the low latitude (including the Southern Hemisphere) SST warming (LLSST response). The tropospheric thermodynamic responses in these experiments reflect global warming, Arctic sea ice loss, and mid-latitude and tropical SST warming (Figure S2). SST and sea-ice boundary data are obtained by averaging over the 30 CMIP5 models (i.e., climatology for the periods 1970–1999 and 2070–2099). The experiments were integrated for 30-year after 1-year spinup. In all of the experiments, radiative forcing is fixed at the 2000 level, following previous studies (Peings & Magnusdottir, 2014; Sun et al., 2015).

For a composite analysis, we have detected latitude of minimum geopotential height at 50 hPa from individual monthly data in HIST experiment. Years with the minimum geopotential height equatorward of 80°N and poleward of 83°N are defined as with and without a polar vortex shift, respectively (Figure S3). We have selected 24 cases with a polar vortex shift toward Eurasia and without a shift.

2.3. LBM Experiments

Atmospheric response to a prescribed diabatic heating was calculated by a linear baroclinic model (LBM) (Watanabe & Kimoto, 2000) with a given climatological basic state and a thermal forcing. A LBM is an important diagnostic tool and widely used to simulate either anomalous or climatological stationary waves. A detailed description of the LBM is found in Watanabe and Kimoto (2000). We here used a spectral resolution of T42 with 20 vertical layers. The vertical maximum of the heating (1 K day^{-1}) is placed at 500 hPa, and the half-width of the horizontal heating pattern is 20° in longitude and 6° in latitude (Yamazaki et al. 2020). The basic state is based on the January climatology (averaged 1979–2010) from the National Centers for Environmental Prediction–National Center for Atmospheric Research (NCEP–NCAR) reanalysis (Kalnay et al., 1996). Although the response to the diabatic heating grows with time, the response pattern does not change much after 10 days. The LBM responses in this study are based on 11–30 day mean.

3. Results

3.1. Future Asymmetry of the Arctic Stratospheric Polar Vortex

In the late 21st century, tropospheric warming and stratospheric cooling are expected in both hemispheres (Figure 1a). However, two major differences are found in both hemispheres, although different seasons: the middle stratospheric cooling above 50 hPa is much weaker in the NH than in the SH, and the lowermost stratospheric cooling at 150–200 hPa is centered on the pole in the SH, whereas in the NH near 60–70°N. The former difference is most pronounced in boreal winter and suggests the competing effects of radiative cooling (Manabe & Wetherald, 1975; Manzini et al., 2014) and dynamical Arctic warming due to a strengthened Brewer-Dobson circulation (Domeisen et al., 2019; Karpechko & Manzini, 2017; Manzini et al., 2014). While the middle stratospheric cooling over the Arctic is the strongest in summer, the lowermost stratospheric cooling only occurs in autumn and winter (Figure 1b), which produce the contrasting temperature responses between the lowermost and middle stratosphere.

Interestingly, in the lowermost (150 hPa) and middle (30 hPa) stratosphere, the Arctic cooling is the strongest over eastern Eurasia, whereas there is little model consensus on the cooling over North America (Figures 1c and 1d). The future changed temperature difference between Eurasia and North America reaches approximately 5°C at 30 hPa, which is responsible for weaker Arctic stratospheric cooling in winter. In the lowermost stratosphere, the Pacific-North American-like (PNA) teleconnection pattern appears to be dominant (Figure 1e). In the middle stratosphere, however, the polar vortex strengthens over Eurasia and weakens over North America, with the eastward shift compared with the climatological wave (Figure 1f), indicating the shift of the polar vortex toward Eurasia (Seviour, 2017; Zhang et al., 2016) or the enhancement of asymmetry between North America and Eurasia. These changes are also confirmed by a Student's t test at the 99% confidence level (Figure S4). The wavenumber 1-like response to climate change has been suggested by some models (Mitchell et al., 2012; Wang & Kushner, 2011), but its cause remains unclear.

3.2. Simulated Polar Vortex Response to Sea Surface Warming

To explore what induces the asymmetric polar vortex response, we make use of existing simulations (Matsumura et al., 2019) with an atmospheric general circulation model (AGCM). Although there are many causes that drive polar vortex variability, such as Arctic sea ice loss, and midlatitude and tropical Pacific warming, our simulations enable to quantify the atmospheric response derived from (a) global SST warming and sea ice loss (GLSST), (b) Arctic sea-ice loss (AICE), (c) midlatitude SST warming (MLSST), and (d) tropical SST warming (LLSST), respectively (see Methods and Figure S2).

First, we discuss the vertical section of the zonal-mean temperature responses (Figures 2a–2d). The simulated GLSST response reproduces well the projected temperature response (Figure 1a), except for the middle stratosphere. The difference between the simulated GLSST and projected model responses is produced by the direct radiative component and ocean-atmosphere coupling (Matsumura et al., 2019). The polar vortex is weakened by AICE and strengthened by MLSST with centered near the pole in the middle stratosphere (Figure S5), which have opposing influences, consistent with previous studies (e.g., Hu et al., 2018; Kim

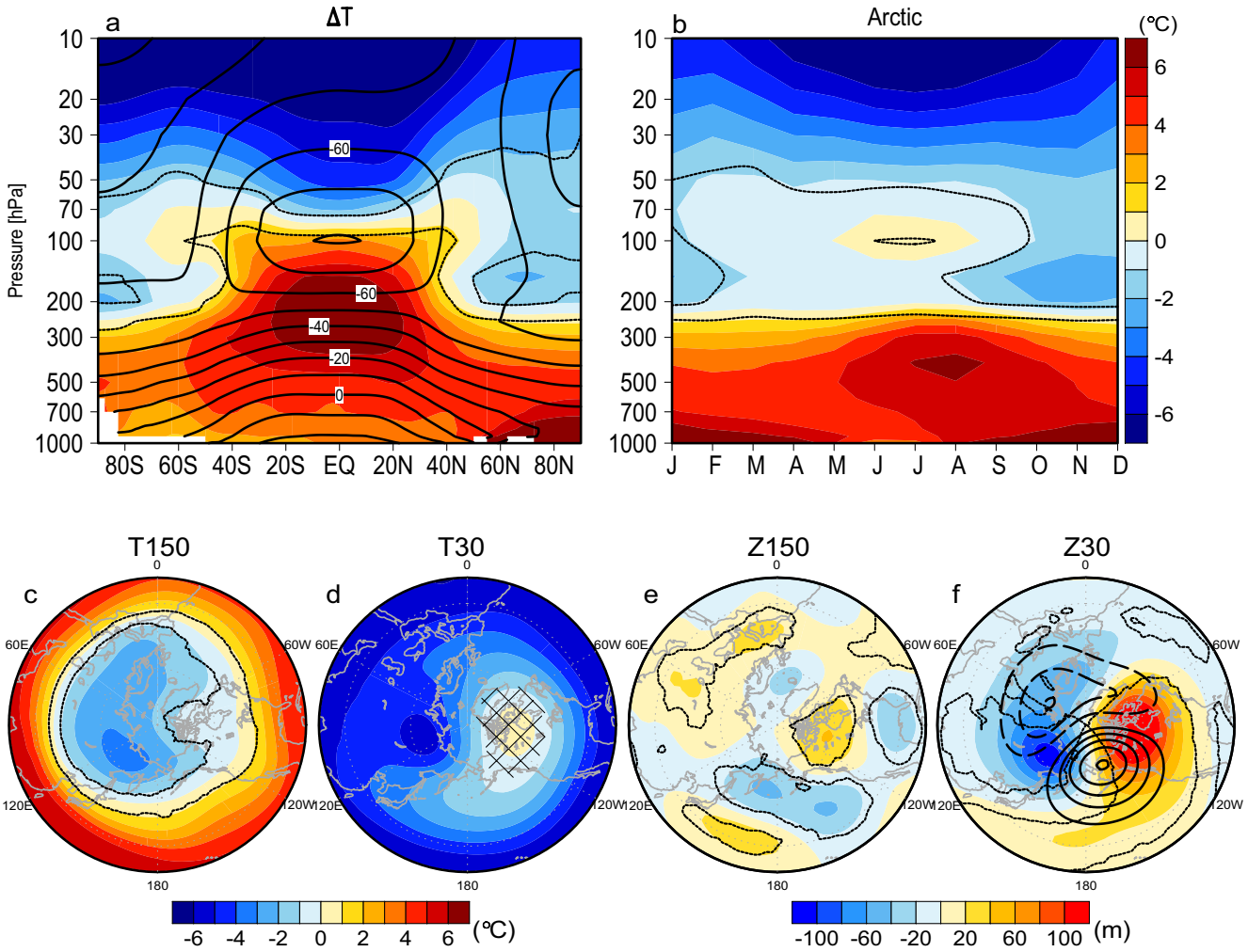

Figure 1. (a) Vertical section of zonal-mean temperature difference between the means over 2070–2099 and 1970–1999 from CMIP5 models in boreal winter (December–February). Solid contours denote the historical temperature climatology (1970–1999). As in (a), but for (b) time-vertical section of the Arctic temperature difference (poleward of 60°N) as a function of calendar month and (c) 150-hPa and (d) 30-hPa temperature differences. (e and f) as in (c and d), but for non-zonal component of geopotential height differences (shaded) and the historical climatology (contour interval is 100 m, with the zero contour omitted; solid for positive and dashed for negative). Dotted contours and hatching indicate ≥80% and <80% model agreement on the sign of the difference, respectively.

et al., 2014; Nakamura et al., 2016; Peings & Magnusdottir, 2014; Sun et al., 2015). The LLSST response captures well the simulated lowermost stratospheric cooling with a peak over 60°–70°N in GLSST, accounting for the projected response. In the GLSST response the lowermost stratospheric cooling from autumn further into spring overestimates the projected response (Figure 1b), due to AICE and MLSST, whereas the LLSST response reproduces well the seasonal evolution. In late winter, however, strong stratospheric warming descends from the middle to the lower stratosphere and is also slightly visible in GLSST, weakening the polar vortex.

Also in the horizontal distributions, the GLSST and LLSST responses capture well the projected lowermost stratospheric cooling with a peak over eastern Eurasia (Figure S6). Surprisingly, in the middle stratosphere, the GLSST and LLSST responses simulate Eurasian cooling and the warming over the North Pacific and North America (Figures 2e and 2f). These results demonstrate that tropical SST warming induces the projected asymmetric temperature response (Figure 1d), independent of the direct radiative cooling effect, Arctic sea ice loss, and midlatitude SST warming. The Eurasian cooling in the lowermost stratosphere is accompanied with a deepened Aleutian low through the PNA pattern (Figure S6), corresponding with the projected circulation response (Figure 1e). In the middle strato-

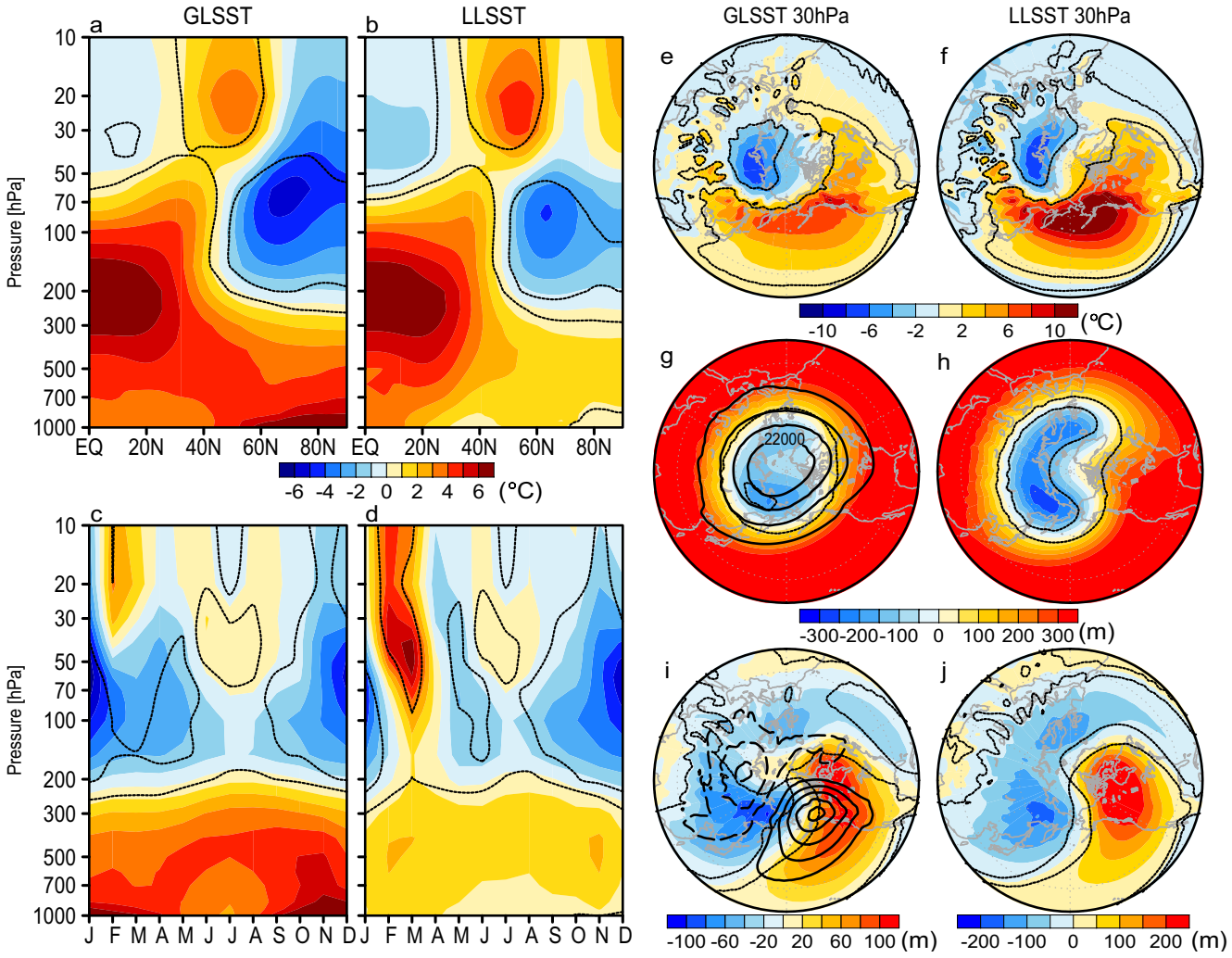

Figure 2. Vertical section of wintertime zonal-mean temperature response in (a) global SST warming and sea ice loss (GLSST) and (b) tropical SST warming (LLSST). (c and d) as in (a and b), but for time-vertical section of the Arctic temperature response. Response of wintertime temperature at 30 hPa in (e) GLSST and (f) LLSST. (g–j) as in (e and f), but for (g, h) geopotential height and (i, j) non-zonal component of geopotential height. Dotted contours indicate statistical significance at the 99% level. Thick contours denote the climatology in HIST experiment (contour interval is 500 m in (g), and 100 m with the zero contour omitted in (i); solid for positive and dashed for negative).

sphere, geopotential height responses show significant decreases over Eurasia along the Arctic coast and increases over North America (Figures 2g and 2h). The wavenumber 1-like responses reproduce well the projected response with the eastward shift compared to the climatological wave (Figures 2i and 2j), leading to the asymmetric polar vortex. These features in GLSST and LLSST correspond well with ENSO impacts on the warming and weakening of the polar vortex; the deepened Aleutian low associated with the positive PNA pattern enhances vertical wave propagation into the stratosphere, which weakens the polar vortex (e.g., Domeisen et al., 2019; Garfinkel & Hartmann, 2008; Ineson & Scaife, 2009; Manzini et al., 2006).

3.3. Role of the Eastern Equatorial Pacific Warming

Returning to the CMIP5 model simulations, in the late 20th century, there are little significant SST correlations with the stratospheric temperatures over North America and Eurasia among the individual models in tropical oceans (Figure S7). In the late 21st century, however, SST correlation with the North American temperature among the individual models positively increases in whole tropical oceans, and the Eurasian

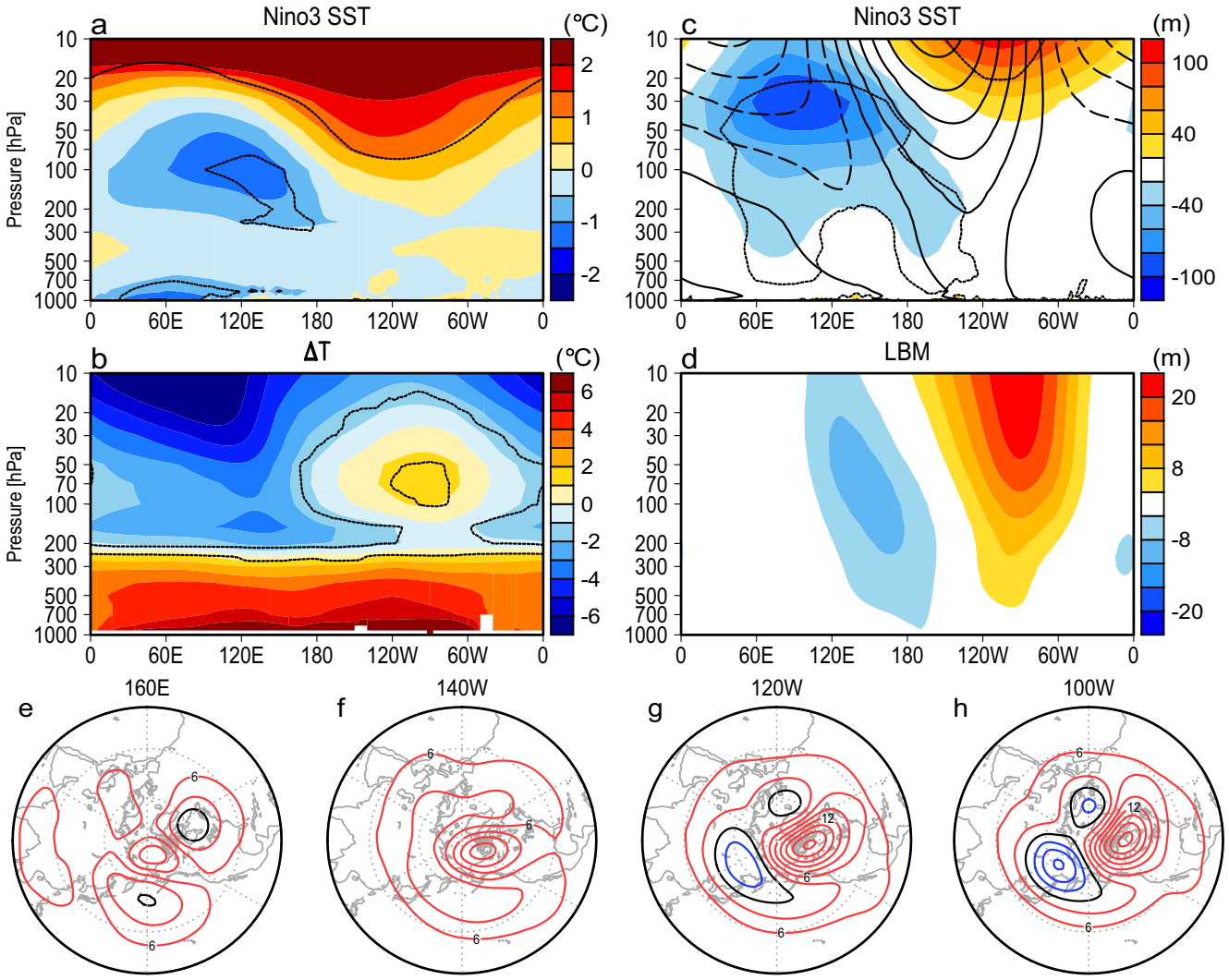

Figure 3. Longitude-vertical section of regressed anomalies of (a) temperature and (c) geopotential height averaged between 60° and 70°N onto standardized Niño-3 SST (5°S–5°N, 90°–150°W) among the individual CMIP5 models in 2070–2099 climatology. (b) As in (a), but for temperature difference between the means over 2070–2099 and 1970–1999. Dotted contours indicate statistical significance over the 95% level in (a and c), and ≥80% model agreement on the sign of the difference in (b). Thick contours in (c) denote the climatological total waves (contour interval is 150 m; solid for positive, dashed for negative, and thick solid for zero). (d) as in (c), but for LBM response to an idealized heating centered over the equator at 100°W. As in (d), but for 30-hPa geopotential height to idealized heating centered over the equator at (e) 160°E, (f) 140°W, (g) 120°W, and (h) 100°W. Contour interval is 3 m; red for positive, blue for negative, and black for the zero contours.

temperature negatively correlates with the western and eastern equatorial Pacific SST (Figure S7). These results support our AGCM simulations that tropical ocean warming induces the asymmetric polar vortex. In particular, the eastern equatorial Pacific, which plays the leading role in ENSO-induced PNA pattern, is expected to most significantly warm in the tropical Pacific (Cai et al., 2015).

Figure 3a shows longitude-vertical section of regressed anomalies of temperature averaged 60°–70°N onto the Niño-3 SST, as a representative of the eastern equatorial Pacific (Domeisen et al., 2019). Eurasian cooling and North American warming are evident, indicating that warmer models in the eastern equatorial Pacific enhance the contrasting temperature response, which is consistent with the projected stratospheric temperature response (Figure 3b). Remarkably, despite the strong radiative cooling, more than 80% of the individual models simulate stratospheric warming over North America approximately 1°C at 70 hPa (Figure 3b), which is consistent across the models (Figure S4). The contrasting temperature response to the Niño-3 SST warming is associated with the asymmetric polar vortex (Figure 3c). The negative geopotential

height anomalies display a westward tilt with altitude roughly from the date line between Eurasia and North America, indicative of vertical wave propagation (Charney & Drazin, 1961). This result implies that the planetary wave response to the Niño-3 SST warming interferes constructively with the climatological wave and enhances vertical wave propagation into the middle stratosphere, similar mechanism to recent shift of the polar vortex toward Eurasia (Zhang et al., 2016).

To validate the asymmetric polar vortex response to the eastern equatorial Pacific warming, we diagnose anomalous planetary waves using a linear baroclinic model (LBM). When an idealized heating is centered over the equator at 100°W under the present climatology, the LBM response also shows a westward tilt with altitude from the date line, enhances vertical wave propagation into the stratosphere, and shifts the polar vortex toward the Eurasian continent, leading to the asymmetric polar vortex with larger amplitude over North America (Figures 3d and 3h). The eastward shifted and deepened Aleutian low through the PNA pattern plays a role in strengthening the planetary wave (Figure S8). Changes in the location or strength of the tropical thermal forcing can considerably affect wave propagation into the stratosphere (Domeisen et al., 2019; Manzini et al., 2006). When the idealized heating is centered at 120°W, the LBM response still shows the asymmetric polar vortex (Figure 3g), but at 140°W in the central Pacific, only weakens the polar vortex (Figure 3f), and at 160°E in the western Pacific, has little influence on the polar vortex (Figure 3e). Consequently, while the deepening of the Aleutian low weakens the polar vortex (Domeisen et al., 2019; Garfinkel & Hartmann, 2008; Ineson & Scaife, 2009), the eastward shift of the Aleutian low leads to the asymmetry by shifting the polar vortex to Eurasia. The eastward-shifted polar vortex response compared with the climatological wave (Figures 1f, 2i, and 3c) is consistent with the eastward shift of the Aleutian low.

In observations, it is difficult to discern the polar vortex responses to the central and eastern Pacific ENSO (Domeisen et al., 2019; Rao & Ren, 2016). In the future, however, the eastward-shifted PNA pattern with the deepened Aleutian low is expected as a robust change (Cai et al., 2015; Gan et al., 2017; Zhou et al., 2014). The eastern equatorial Pacific warms faster than the surrounding regions (Cai et al., 2015), exceeding the SST threshold for tropical convection (Johnson & Xie, 2010; Zhou et al., 2014), which in turn induces the eastward-shifted PNA pattern and leads to the asymmetric polar vortex. Indeed, both coupled (CMIP5) models and our AGCM simulations indicate equatorial wave response over the eastern tropical Pacific (Figure S9), as a result of increased precipitation in a comparable magnitude with the central equatorial Pacific (Figure S10).

4. Summary and Discussion

We have addressed the question that if the observed asymmetry of the polar vortex continues into the future, what might be the relevant cause? There was no robust consensus on the response of the polar vortex to climate change among the CMIP5 models (Manzini et al., 2014; Simpson et al., 2018). We find that over North America, the Arctic stratospheric cooling is suppressed or rather warming occurs, whereas over Eurasia stratospheric cooling is most pronounced, leading to an asymmetric polar vortex. The North American stratospheric warming explodes the established understanding in a warming climate. The eastern equatorial Pacific warming plays the role in strengthening the polar vortex over Eurasia and weakening over North America.

The observed asymmetric polar vortex begins to develop in the late 20th century (Seviour, 2017; Zhang et al., 2016). The multi-model mean appears to capture recent weakening and shift of the polar vortex, and then the weakening becomes moderate by the 2030s (Figure 4b), possibly due to the opposing effects of Arctic sea ice loss (e.g., Kim et al., 2014; Nakamura et al., 2016; Peings & Magnusdottir, 2014; Sun et al., 2015) and midlatitude SST warming (Hu et al., 2018) (Figure S5), although unforced internal variability might be sufficiently strong (Garfinkel et al., 2017; Screen et al., 2018; Seviour, 2017). From the 2030s, however, the polar cap height rapidly increases over North America and decreases over Eurasia, asymmetrically enhancing the polar vortex. While Eurasian cooling increasingly becomes strong, North American cooling is suppressed and maintained close to the present temperature by 2100 (Figure 4a). This rapid change in the 2030s suggests that tropical Pacific warming takes the place of Arctic sea ice loss and midlatitude SST warming as the dominating forcing of the polar vortex.

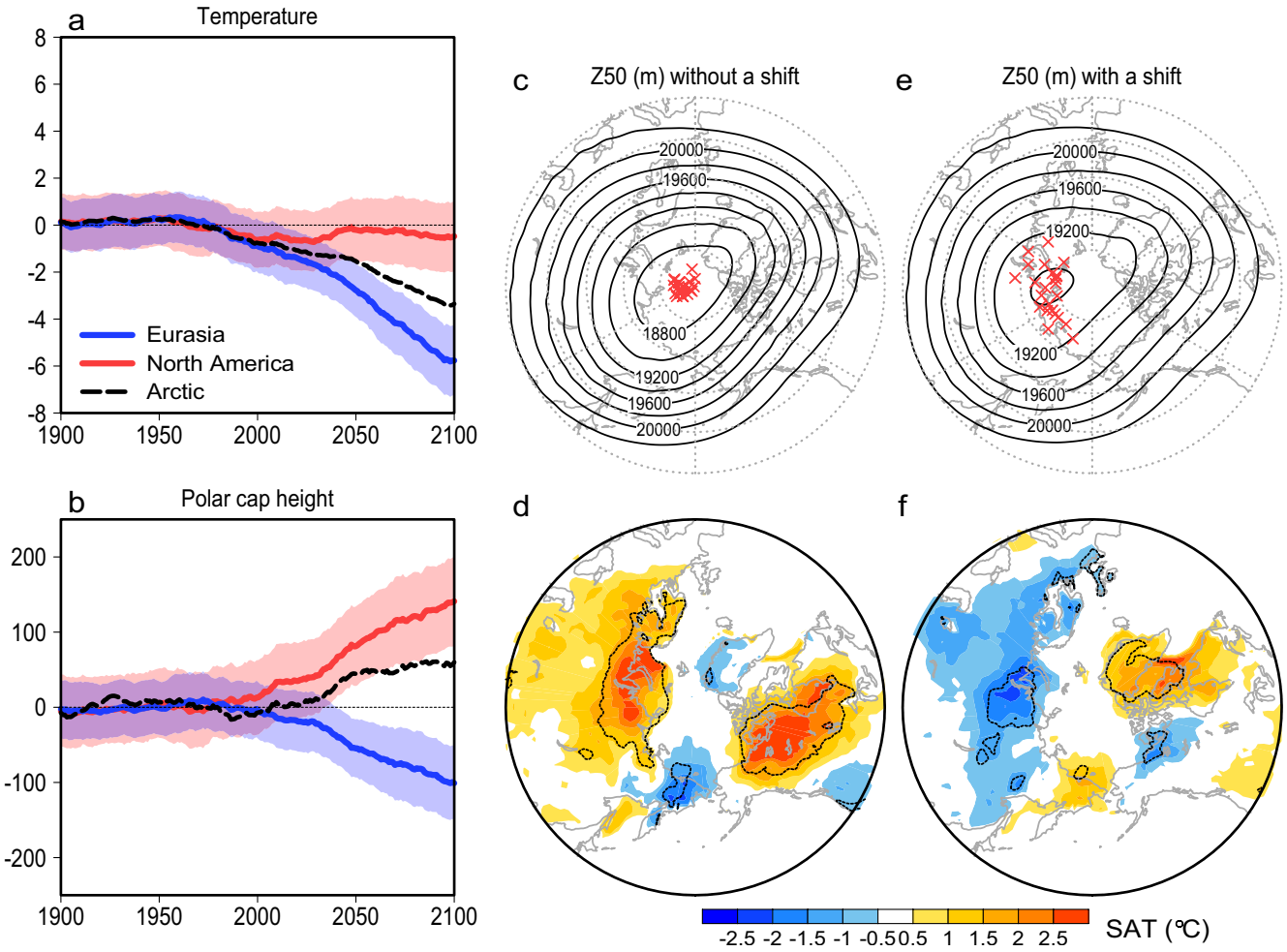

Figure 4. Time series of 50–10 hPa mean (a) temperature (°C) and (b) polar cap height (m) anomalies over Eurasia (100°–150°E, 60°–70°N; blue line), North America (60°–110°W, 60°–70°N; red line), and the Arctic (poleward of 60°N; black dashed line) from 1900 to 2100, relative to the 1901–2000 mean. All the lines and shadings indicate the multi-model mean and ±2 standard error (95% confidence range) among the models, respectively, with 21-year running means. Composite mean of 50-hPa geopotential height (m) for the years (c) without and (e) with a polar vortex shift toward Eurasia, based on HIST experiment. Red crosses denote a position of minimum geopotential height. (d and f) As in (c and e), but for composite mean anomalies with 30-year ensemble mean in surface air temperature (°C). Dotted contours indicate statistical significance at the 95% level.

The stratospheric variations can have a strong impact on surface weather and climate through the stratosphere-troposphere coupling (e.g., Baldwin & Dunkerton, 2001; Ineson & Scaife, 2009). In the late 21st century, subseasonal surface temperature variability (i.e., cold extremes) is projected to significantly decrease over the mid- to high-latitude NH due to Arctic amplification (Screen, 2014). However, the cold extremes are likely to increase during a few decades from the 2030s (see Figure 4 of Screen, 2014). Despite recent debate on the impact of Arctic sea ice loss (Screen et al., 2018), in a few decades, the asymmetric polar vortex could act to increase the cold extreme events, such as recent cold-air-outbreak over Eurasia (Kretschmer et al., 2018). Indeed, composite analysis based on AGCM simulations shows that surface cooling (warming) is enhanced over Eurasia, including Europe, associated with a polar vortex shift toward Eurasia (no shift) (Figures 4c–4f), indicative of a negative (positive) Arctic Oscillation. In particular, the surface cooling is pronounced over Eurasia, but not over North America. Our results here provide a new insight into Arctic climate changes and important implications for the near future projection on surface climate. Contrary to highly uncertain future projection in the zonal mean response of the polar vortex (Manzini et al., 2014; Screen et al., 2018; Simpson et al., 2018), the asymmetry is a robust change to be expected in the future.

Data Availability Statement

The CMIP5 datasets can be downloaded from the Earth System Grid Federation at https://pcmdi.llnl.gov/mips/cmip5/. Part of the AGCM simulations was conducted by S. Ueki (Matsumura et al. 2019). DCPAM5 is available from http://www.gfd-dennou.org/library/dcpam/index.htm.en.

Acknowledgments
We acknowledge the WCRP's Working Group on Coupled Modeling and thank the climate modeling groups (Table S1) for producing and making available their model output. Koji Yamazaki was supported by the Arctic Challenge for Sustainability (ArCS) program in Japan and Japan Arctic Research Network Center (J-ARC Net). Takeshi Horinouchi was supported by the Environment Research and Technology Development Fund (2-1904) of Environmental Restoration and Conservation Agency, Japan.

References

Baldwin, M. P., & Dunkerton, T. J. (2001). Stratospheric harbingers of anomalous weather regimes. *Science*, *294*, 581–584. https://doi.org/10.1126/science.1063315

Cai, W., Santoso, A., Wang, G., Yeh, S.-W., An, S.-I., Cobb, K. M., et al. (2015). ENSO and greenhouse warming. *Nature Climate Change*, *5*, 849–859. https://doi.org/10.1038/nclimate2743

Charney, J. G., & Drazin, P. G. (1961). Propagation of planetary scale disturbances from the lower into the upper atmosphere. *Journal of Geophysical Research*, *66*, 83–109. https://doi.org/10.1029/jz066i001p00083

Domeisen, D. I., Garfinkel, C. I., & Butler, A. H. (2019). The teleconnection of El Niño Southern Oscillation to the stratosphere. *Reviews of Geophysics*, *57*, 5–47. https://doi.org/10.1029/2018rg000596

Gan, B., Wu, L., Jia, F., Li, S., Cai, W., Nakamura, H., et al. (2017). On the response of the Aleutian low to greenhouse warming. *Journal of Climate*, *30*, 3907–3925. https://doi.org/10.1175/jcli-d-15-0789.1

Garfinkel, C. I., & Hartmann, D. L. (2008). Different ENSO teleconnections and their effects on the stratospheric polar vortex. *Journal of Geophysical Research*, *113*, 1044. https://doi.org/10.1029/2008jd009920

Garfinkel, C. I., Son, S.-W., Song, K., Aquila, V., & Oman, L. D. (2017). Stratospheric variability contributed to and sustained the recent hiatus in Eurasian winter warming. *Geophysical Research Letters*, *44*, 374–382. https://doi.org/10.1002/2016gl072035

Hu, D., Guan, Z., Tian, W., & Ren, R. (2018). Recent strengthening of the stratospheric Arctic vortex response to warming in the central North Pacific. *Nature Communications*, *9*, 1697. https://doi.org/10.1038/s41467-018-04138-3

Ineson, S., & Scaife, A. (2009). The role of the stratosphere in the European climate response to El Niño. *Nature Geoscience*, *2*, 32–36. https://doi.org/10.1038/ngeo381

Johnson, N. C., & Xie, S. P. (2010). Changes in the sea surface temperature threshold for tropical convection. *Nature Geoscience*, *3*, 842–845. https://doi.org/10.1038/ngeo1008

Kalnay, E., Kanamitsu, M., Kistler, R., Collins, W., Deaven, D., Gandin, L., et al. (1996). The NCEP/NCAR 40-year reanalysis project. *Bulletin of the American Meteorological Society*, *77*, 437–471. https://doi.org/10.1175/1520-0477(1996)077<0437:tnyrp>2.0.co;2

Karpechko, A. Y., & Manzini, E. (2017). Arctic stratosphere dynamical response to global warming. *Journal of Climate*, *30*, 7071–7086. https://doi.org/10.1175/jcli-d-16-0781.1

Kim, B. M., Son, S.-W., Min, S.-K., Jeong, J.-H., Kim, S.-J., Zhang, X., et al. (2014). Weakening of the stratospheric polar vortex by Arctic sea-ice loss. *Nature Communications*, *5*, 4646. https://doi.org/10.1038/ncomms5646

Kim, J., Son, S., Gerber, E. P., & Park, H. (2017). Defining sudden stratospheric warming in climate models: Accounting for biases in model climatologies. *Journal of Climate*, *30*, 5529–5546. https://doi.org/10.1175/jcli-d-16-0465.1

Kobayashi, S., Ota, Y., Harada, Y., Ebita, A., Moriya, M., Onoda, H., et al. (2015). The JRA-55 reanalysis: General specifications and basic characteristics. *Journal of the Meteorological Society of Japan*, *93*, 5–48. https://doi.org/10.2151/jmsj.2015-001

Kretschmer, M., Coumou, D., Agel, L., Barlow, M., Tziperman, E., & Cohen, J. (2018). More-persistent weak stratospheric polar vortex states linked to cold extremes. *Bulletin of the American Meteorological Society*, *99*, 49–60. https://doi.org/10.1175/bams-d-16-0259.1

Manabe, S., & Wetherald, R. T. (1975). The effects of doubling the CO2 concentration on the climate of a General Circulation Model. *Journal of the Atmospheric Sciences*, *32*, 3–15. https://doi.org/10.1175/1520-0469(1975)032<0003:teodtc>2.0.co;2

Manzini, E., Giorgetta, M. A., Esch, M., Kornblueh, L., & Roeckner, E. (2006). The Influence of sea surface temperatures on the Northern Winter Stratosphere: Ensemble simulations with the MAECHAM5 Model. *Journal of Climate*, *19*, 3863–3881. https://doi.org/10.1175/jcli3826.1

Manzini, E., Karpechko, A. Y., Anstey, J., Baldwin, M. P., Black, R. X., Cagnazzo, C., et al. (2014). Northern winter climate change: Assessment of uncertainty in CMIP5 projections related to stratosphere–troposphere coupling. *Journal of Geophysical Research*, *119*, 7979–7998. https://doi.org/10.1002/2013jd021403

Matsumura, S., Ueki, S., & Horinouchi, T. (2019). Contrasting responses of mid-latitude jets to the North Pacific and North Atlantic warming. *Geophysical Research Letters*, *46*, 3973–3981. https://doi.org/10.1029/2019gl082550

Mitchell, D. M., Osprey, S. M., Gray, L. J., Butchart, N., Hardiman, S. C., Charlton-Perez, A. J., & Watson, P. (2012). The effect of climate change on the variability of the Northern Hemisphere Stratospheric polar vortex. *Journal of the Atmospheric Sciences*, *69*, 2608–2618. https://doi.org/10.1175/jas-d-12-021.1

Nakamura, T., Yamazaki, K., Iwamoto, K., Honda, M., Miyoshi, Y., Ogawa, Y., et al. (2016). The stratospheric pathway for Arctic impacts on midlatitude climate. *Geophysical Research Letters*, *43*, 3494–3501. https://doi.org/10.1002/2016gl068330

Peings, Y., & Magnusdottir, G. (2014). Response of the wintertime Northern Hemisphere atmospheric circulation to current and projected Arctic sea ice decline: A numerical study with CAM5. *Journal of Climate*, *27*, 244–264. https://doi.org/10.1175/jcli-d-13-00272.1

Rao, J., & Ren, R. (2016). Asymmetry and nonlinearity of the influence of ENSO on the northern winter stratosphere: 1. Observations. *Journal of Geophysical Research*, *121*, 9000–9016. https://doi.org/10.1002/2015jd024520

Screen, J. A. (2014). Arctic amplification decreases temperature variance in northern mid- to high-latitudes. *Nature Climate Change*, *4*, 577–582. https://doi.org/10.1038/nclimate2268

Screen, J. A., Bracegirdle, T. J., & Simmonds, I. (2018). Polar climate change as manifest in atmospheric circulation. *Current Climate Change Reports*, *4*, 383–395. https://doi.org/10.1007/s40641-018-0111-4

Seviour, W. J. M. (2017). Weakening and shift of the Arctic stratospheric polar vortex: Internal variability or forced response? *Geophysical Research Letters*, *44*, 3365–3373. https://doi.org/10.1002/2017gl073071

Simpson, I. R., Hitchcock, P., Seager, R., Wu, Y., & Callaghan, P. (2018). The downward influence of uncertainty in the Northern Hemisphere Stratospheric polar vortex response to climate change. *Journal of Climate*, *31*(16), 6371–6391. https://doi.org/10.1175/jcli-d-18-0041.1

Sun, L., Deser, C., & Tomas, R. A. (2015). Mechanisms of stratospheric and tropospheric circulation response to projected Arctic sea ice loss. *Journal of Climate*, *28*, 7824–7845. https://doi.org/10.1175/jcli-d-15-0169.1

Takahashi, Y. O., & DCPAM Development Group. (2018). *DCPAM: Planetary atmosphere model*. Retrieved from http://www.gfd-dennou.org/library/dcpam/index.htm.en

Taylor, K. E., Stouffer, R. J., & Meehl, G. A. (2012). An overview of CMIP5 and the experiment design. *Bulletin of the American Meteorological Society*, *93*, 485–498. https://doi.org/10.1175/bams-d-11-00094.1

Wang, L., & Kushner, P. J. (2011). Diagnosing the stratosphere-troposphere stationary wave response to climate change in a general circulation model. *Journal of Geophysical Research*, *116*, D16113. https://doi.org/10.1029/2010jd015473

Watanabe, M., & Kimoto, M. (2000). Atmosphere-ocean thermal coupling in the North Atlantic: A positive feedback. *The Quarterly Journal of the Royal Meteorological Society*, *126*, 3343–3369. https://doi.org/10.1002/qj.49712657017

Waugh, D., Sobel, A. H., & Polvani, L. M. (2017). What is the polar vortex and how does it influence weather? *Bulletin of the American Meteorological Society*, *98*, 37–44. https://doi.org/10.1175/bams-d-15-00212.1

Yamazaki, K., Nakamura, T., Ukita, J., & Hoshi, K. (2020). A tropospheric pathway of the stratospheric oscillation (QBO) impact on the boreal winter polar vortex. *Atmospheric Chemistry and Physics*, *20*, 5111–5127. https://doi.org/10.5194/acp-20-5111-2020

Zhang, J., Tian, W., Xie, F., Chipperfield, M. P., Feng, W., Son, S.-W., et al. (2018). Stratospheric ozone loss over the Eurasian continent induced by the polar vortex shift. *Nature Communications*, *9*, 206. https://doi.org/10.1038/s41467-017-02565-2

Zhang, J., Wenshou, T., Chipperfield, M. P., Xie, F., & Huang, J. (2016). Persistent shift of the Arctic polar vortex toward the Eurasian continent in recent decades. *Nature Climate Change*, *6*, 1094–1099. https://doi.org/10.1038/nclimate3136

Zhou, Z., Xie, S.-P., Zheng, X., Liu, Q., & Wang, H. (2014). Global warming–induced changes in El Niño teleconnections over the North Pacific and North America. *Journal of Climate*, *27*, 9050–9064. https://doi.org/10.1175/jcli-d-14-00254.1